Progress In Electromagnetics Research M, Vol. 120, 179–189, 2023

A Wideband High-Gain Antenna Loaded with Triangular Ring Metasurface

Ting Wu*, Jia-Wei Wang, Ming-Jun Wang, and Kai Zhang

Abstract—A broadband high gain antenna based on metasurface is proposed in this paper. The antenna consists of two layers. The lower layer is a 64 mm × 64 mm square substrate, which is fed through aperture coupling to bring the resonant frequencies closer to each other to increase the bandwidth. The upper layer is a substrate of the same size, and the substrate is covered with a metasurface composed of 4×4 triangular slots. The impedance bandwidth is expanded by introducing the metasurface from 6.7% of the single-feed antenna(without metasurface) to 23.8%, and the overall height of the antenna is 7 mm. The antenna is excited by an aperture-coupled structure consisting of a microstrip line on the back and a narrow slot etched on the ground surface. The impedance bandwidth of the proposed antenna is 23.8%, ranging from 4.8 GHz to 6.1 GHz. The peak gain at 5.6 GHz is about 11.2 dB, which is relatively stable throughout the operating frequency band. An antenna prototype is made, and the measurement results verify the design's correctness.

1. INTRODUCTION

In modern society, communication technology is developing rapidly, and antennas play an important role in their performance directly affecting communication quality and efficiency. Therefore, the requirements for antennas are becoming increasingly high nowadays. Microstrip patch antennas have a narrow impedance bandwidth, but their small size and low cost make them widely used. How to broaden their bandwidth has become a hot topic. In [1–4], the bandwidth is broadened by cutting different shape slots based on antennas. After analysis and verification, they have achieved their desired results and have been applied to different communication frequency bands. Metamaterial is an artificial electromagnetic material with extraordinary physical properties, which are not possessed by natural materials [5]. A metasurface (MS) is a two-dimensional surface structure of metamaterial, which has the same effect as metamaterial. Papers [6–9] cover different shapes of metasurfaces on antennas to expand bandwidth or achieve different polarization methods and various performances. In summary, there have been significant breakthroughs in the study of the combination of metasurfaces and antennas. Combining the two technologies will provide more ideas for antenna design and improve the performance indicators of antennas.

In paper [10], a grid-type metasurface is loaded on a patch antenna to realize the control of the antenna wave beam direction. In paper [11], a rectangular square metasurface is loaded on an antenna, which makes the antenna bandwidth reach 28% and improves the gain. Paper [12] covers an antenna with rectangular metasurfaces of varying sizes, resulting in a bandwidth of 67.3%, named as ultra-wideband antenna, with a gain of 9.18 dB. In paper [13], a new high-gain Fabry-Perot antenna is proposed, which is loaded with a part of the reflective surface of a single layer of metamaterial. The results show that the gain is up to 8.2 dB, 150% more than the feed antenna gain, and the impedance bandwidth is up to 15.5%. In summary, metasurface plays a good role in improving antenna gain, but with the complexity

Received 29 August 2023, Accepted 30 September 2023, Scheduled 7 November 2023
* Corresponding author: Ting Wu (wutingzdh@xaut.edu.cn).
The authors are with the School of Automation and Information Engineering, Xi'an University of Technology, Xi'an 710048, China.

of the electromagnetic environment, how to improve the bandwidth of the antenna has become an urgent problem.

In paper [14], a new defect ground structure is used to achieve broadband, and a reflector is used to improve the antenna gain. The final antenna coverage is 4.9–5.8 GHz with a maximum gain of 6.21 dB. Paper [15] loads a double-layer metasurface, fed by the lowest aperture coupling, and ultimately operates at 4.08–6.38 GHz with a peak gain of 11.6 dB. However, its high-frequency gain cannot be maintained at a high level, and this type of antenna can still be further explored to improve performance. Paper [16] proposes a double mushroom array, which excites a new resonant mode. The final impedance bandwidth is 11.9–18.2 GHz, covering the entire Ku band, and has a stable gain of 10–10.5 dB. The above work provides a promising method for improving antenna bandwidth and high gain, but there are still some problems such as complicated design, low gain, and instability.

At present, the research on metasurfaces mainly includes in-depth theoretical research on the physical properties of metasurfaces, continued exploration of various forms of metasurface structures in structure, and continued research on the applications of metasurfaces in antennas and other fields in applications. In the past decade, metamaterials have shifted from a purely theoretical concept to a field with product development and market applications. The physical properties of three-dimensional metamaterials can be achieved by arranging small-size electromagnetic scatterers or holes into a two-dimensional plane structure on the surface or interface of an object. The two-dimensional flat version of this metamaterial has been named 'metasurface'. Due to its advantage of occupying small physical space, metasurfaces have replaced three-dimensional metamaterial structures in many small-scale application scenarios. Metasurfaces have a wide range of potential applications in electromagnetics, mainly including: reducing the radar cross section (RCS) of antennas by metasurfaces, achieving polarization conversion by metasurfaces, and increasing antenna bandwidth by metasurfaces. Paper [17] by loading non-periodic metasurface structures achieves a wide impedance bandwidth above 79% and a wide 3 dB realized gain bandwidth of 77%. In paper [18], a miniaturized MS structure using via-wall capacitive loading is investigated, and the proposed miniaturized patch-via-wall MS structure is applied to realize a compact wideband antenna fed by a microstrip line through a coupling slot to achieve a large impedance bandwidth. In paper [19], the antenna configuration is a square-modified microstrip patch sandwiched between a metasurface and the ground plane. The metasurface comprises a 4×4 array of square patches, while the single-feed radiating microstrip patch has axial ratio (AR) tuning stubs and a crossed slot. It has a measured 3 dB gain bandwidth of 5.17–8.2 GHz (45.32%), with a measured peak gain of 12.17 dBic. In this paper, a 4×4 metasurface array composed of triangular ring elements is presented and compared with the traditional rectangular array metasurface, explained, and the superior performance of metasurfaces is analyzed using this structure.

Inspired by these works, this article proposes a patch antenna with a simple design, broadband, and high gain loaded triangular ring metasurface structure. By loading the 4×4 triangular toroidal metasurface, the current loss radiation is reduced. Compared with the traditional rectangular patch antenna, the bandwidth can reach 23.8%, operating at 5.8 GHz, which is applied to the WLAN band. The experimental results show that the antenna can achieve an impedance bandwidth of 23.8% (4.8–6.1 GHz) and a gain peak up to 11.2 dB.

2. ANTENNA DESIGN AND ANALYSIS

2.1. Antenna Design and Structure

The structure of the antenna is shown in Figure 1, and the antenna is composed of two substrates. The upper patch is etched on the upper surface of the top layer, as shown in Figure 1(a). The antenna is fed by a 50 Ω Microstrip line through the center of the slot etched on the ground plane so that two adjacent resonance modes will be excited. The antenna is designed on a Rogers RO4003 substrate with a thickness of 1.5 mm. The metasurface antenna is excited by an aperture-coupled structure located below the metasurface. The structure is composed of a microstrip line and a narrow slot etched on the ground plane, as shown in Figures 1(b) and (c).

The final parameters of the antenna are as follows: $L_1 = L_2 = 64$ mm, the $F_s = 36$ mm, $F_w = 7$ mm, $S_{L1} = 32$ mm, $S_{L2} = 7$ mm, $S_{W1} = 3$ mm, $S_{W2} = 4$ mm, $S_1 = 12$ mm, $S_2 = 6$ mm, $g_1 = 2$ mm,

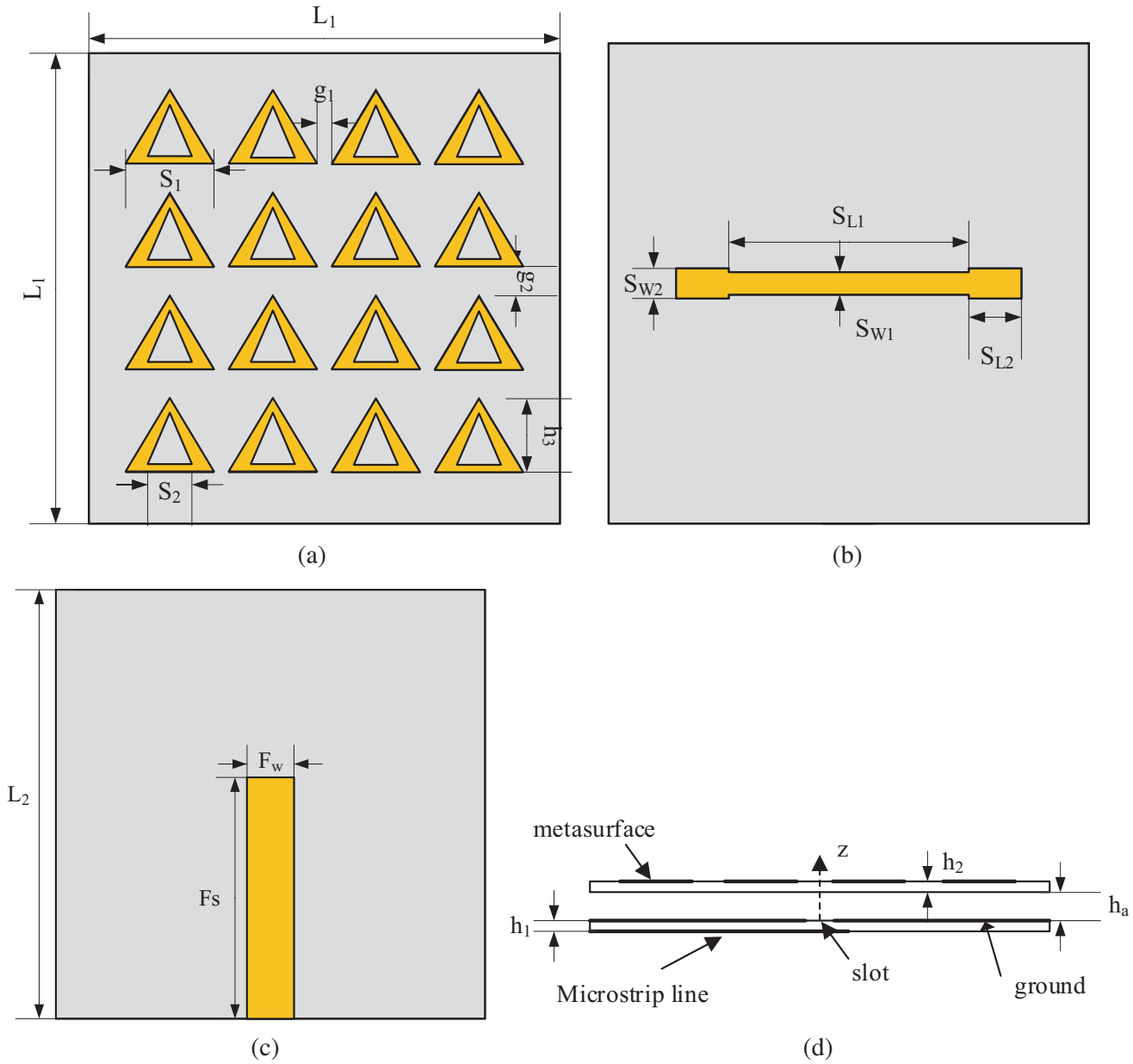

Figure 1. Configuration of the proposed antenna. (a) Top view. (b) Upper surface view of the bottom layer. (c) Bottom view. (d) Side view.

$g_2 = 4\,\text{mm}$, $h_1 = h_2 = 1.5\,\text{mm}$, $h_3 = 10\,\text{mm}$, $h_a = 4\,\text{mm}$. The antenna is simulated using three-dimensional electromagnetic simulation software (HFSS). The simulated S_{11} is shown in Figure 2(a), and the gain is shown in Figure 2(b).

The metasurface is composed of 16 triangular ring slots of the same size. The simulation compares metasurfaces of the same size with and without slotting. Due to similar slotting treatment, the antenna bandwidth is widened. The S_{11} and gain curves of the two antennas are compared through simulation as shown in Figure 3.

Figure 3 shows that S_{11} is wider and better matched, and the gain is also 1 dB higher after cutting slots on the triangular metasurface.

Then we simulate a traditional rectangular metasurface antenna of the same size and analyze its S_{11} and gain, as shown in Figure 4. Its structure is shown in Figure 5. The traditional rectangular

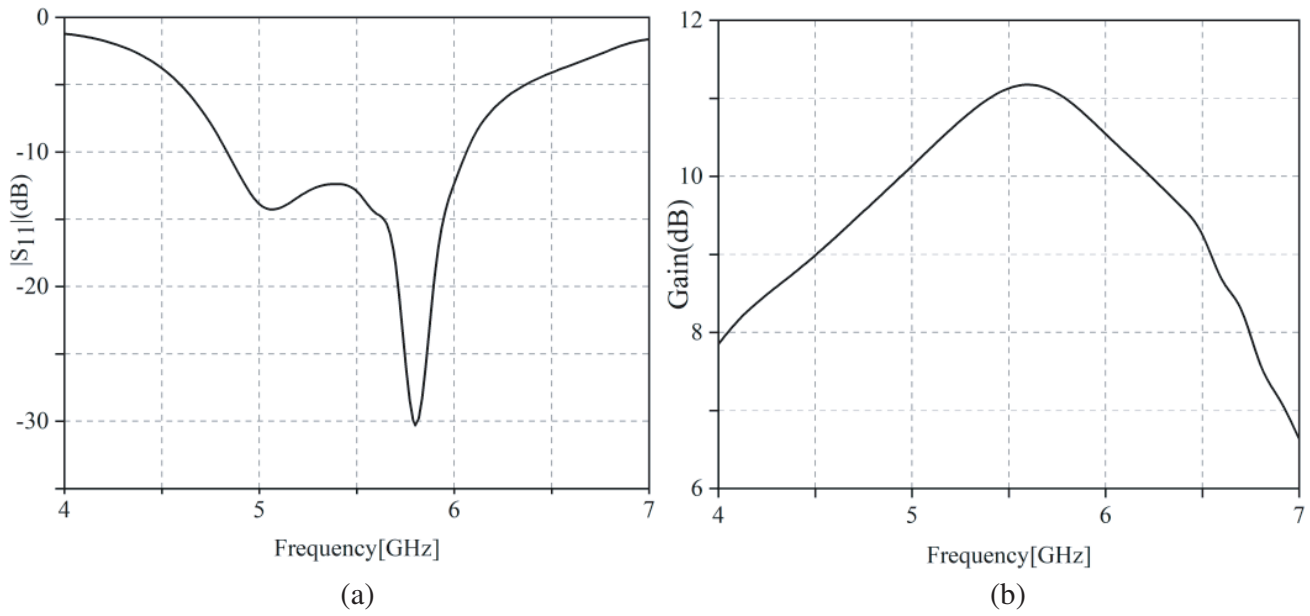

Figure 2. Simulated S_{11} and Gain of the antenna. (a) S_{11}. (b) Gain.

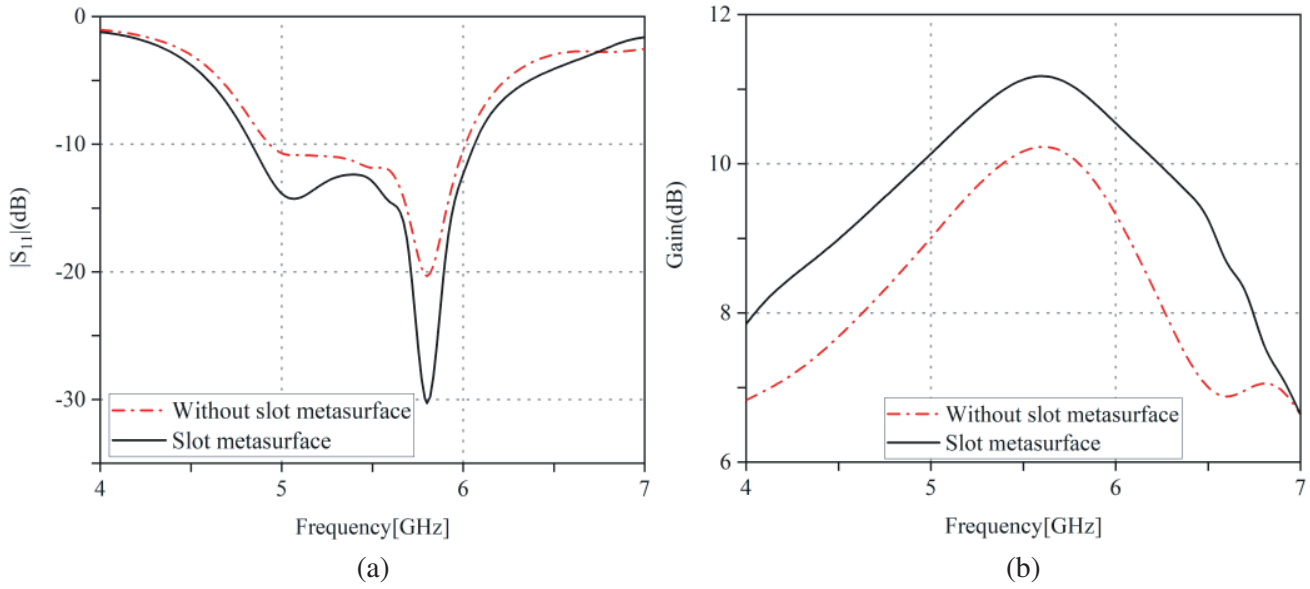

Figure 3. Slot and without slot metasurface S_{11} and Gain. (a) S_{11} comparison. (b) Gain comparison.

metasurface antenna works between 5.7 and 6.1 GHz, and its gain decreases from 11.2 dB to 9.4 dB in the operating frequency range, with the gain jitter in the high-frequency range. Its performance is not as good as the triangular ring-type metasurface antenna proposed in the paper.

Then we simulate a single feed antenna, as shown in Figure 6. A single feed antenna is the lower layer structure left behind after removing the upper metasurface structure. Its structure is shown in Figure 7. It can be seen from Figure 5 that the bandwidth of the single feed antenna is 5.8–6.1 GHz, and the gain is only 3 dB and soon drops to 0, far lower than the performance after loading the metasurface, which can explain the influence of the metasurface on the performance of the antenna. Compared with the triangular metasurface, it works at 4.8–6.1 GHz, enlarging the working bandwidth, and the peak

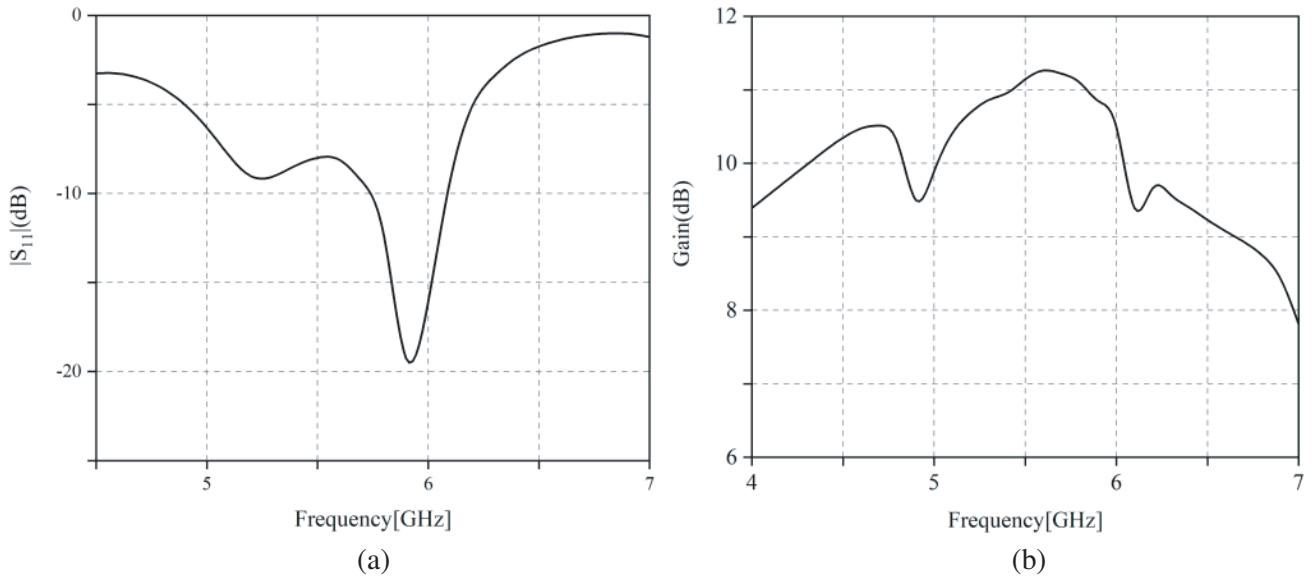

Figure 4. Simulated S_{11} and Gain results of the rectangular metasurface. (a) S_{11}. (b) Gain.

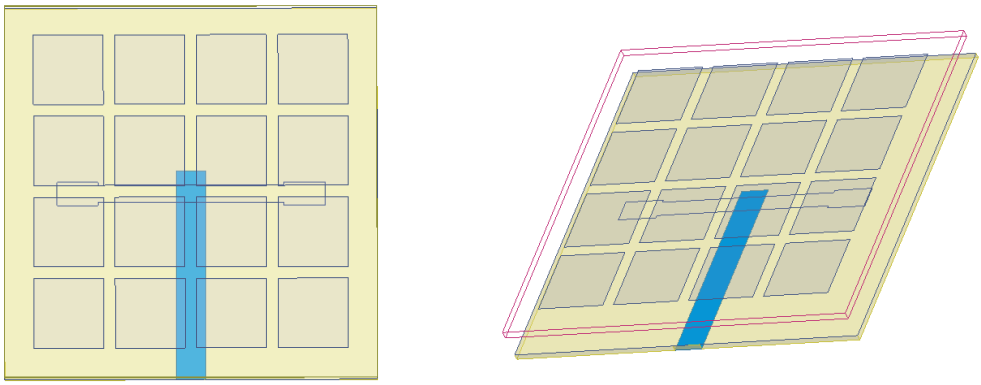

Figure 5. The rectangular metasurface antenna structure.

gain reaches 11.2 dB, but it can be maintained at a high level, achieving the role of enhancing bandwidth and gain.

2.2. Parameter Study

To improve the performance of the antenna, the parameter simulation analysis of each parameter of the antenna is carried out. Through simulation analysis, the antenna size was finally determined to be 64 × 64 mm, and then all other parameters were simulated and analyzed. For the whole antenna, only one parameter is changed each time, and other parameters remain unchanged. Select the three or four parameters with the greatest influence. After a large number of scanning of various antenna parameters, we found that the height of the air layer 'H_a', the length of the feeder 'F_s', and the length and width of the slot 'S_{L1}' 'S_{W1}' have the greatest impact on antenna performance. On this basis, a large number of specific values of these parameters were selected for simulation. The values presented in front of you are the values that have the most impact on antenna performance, so finally select the values. The analysis is given below.

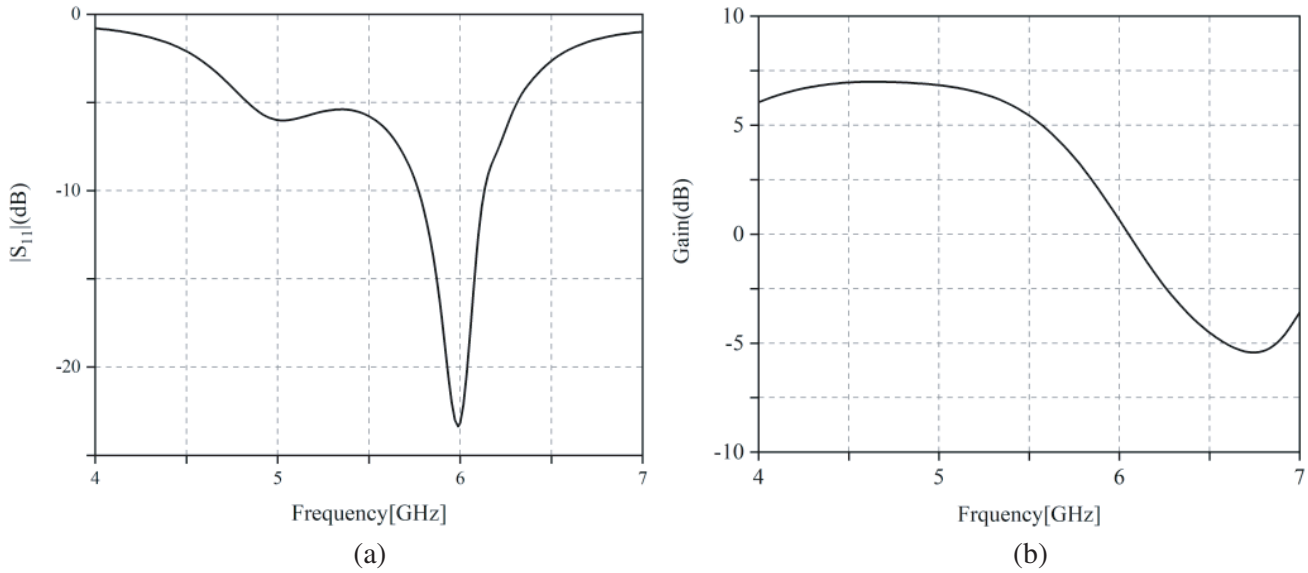

Figure 6. Simulated S_{11} and Gain results of the single feed antenna. (a) S_{11}. (b) Gain.

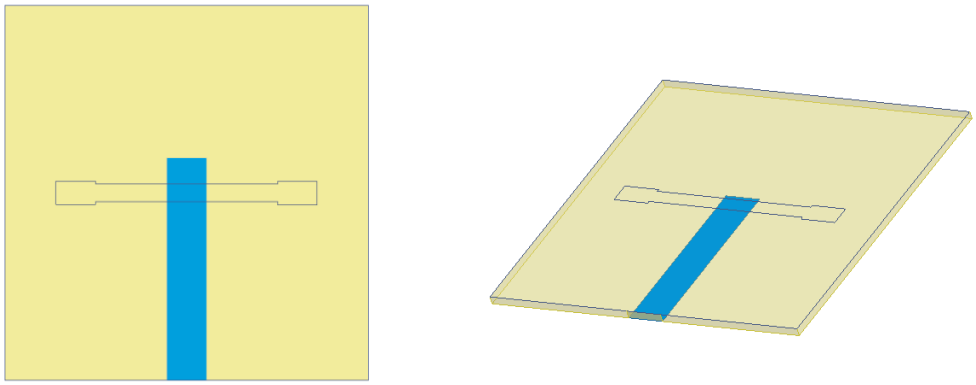

Figure 7. The single-feed antenna structure.

2.2.1. Effect of H_a

For the first time, the height H_a between two boards was changed, and the effect of different cavity heights on bandwidth and gain performance was studied, while other parameters remained unchanged. The range of H_a values selected is 2–5 mm, and simulation is conducted every 1 mm of interval. Figure 8 shows the changes in S_{11} and gain curves corresponding to four different values.

When H_a increases, the impedance matching is better, and the resonance point remains unchanged at 5.8 GHz. When $H_a = 3$ or 4 mm, the antenna has better impedance matching and the widest bandwidth. When $H_a = 4$ mm, the gain of the antenna is relatively high and stable, so $H_a = 4$ mm is chosen.

2.2.2. Effect of Microstrip Line Size

Then, the parameter simulation of feeder length F_s was carried out to study the influence of different feeder lengths on bandwidth performance. The F_s value range was selected to be 36–42 mm, and the simulation was performed at an interval of 2 mm. Figure 9 shows the impact of F_s on S_{11}.

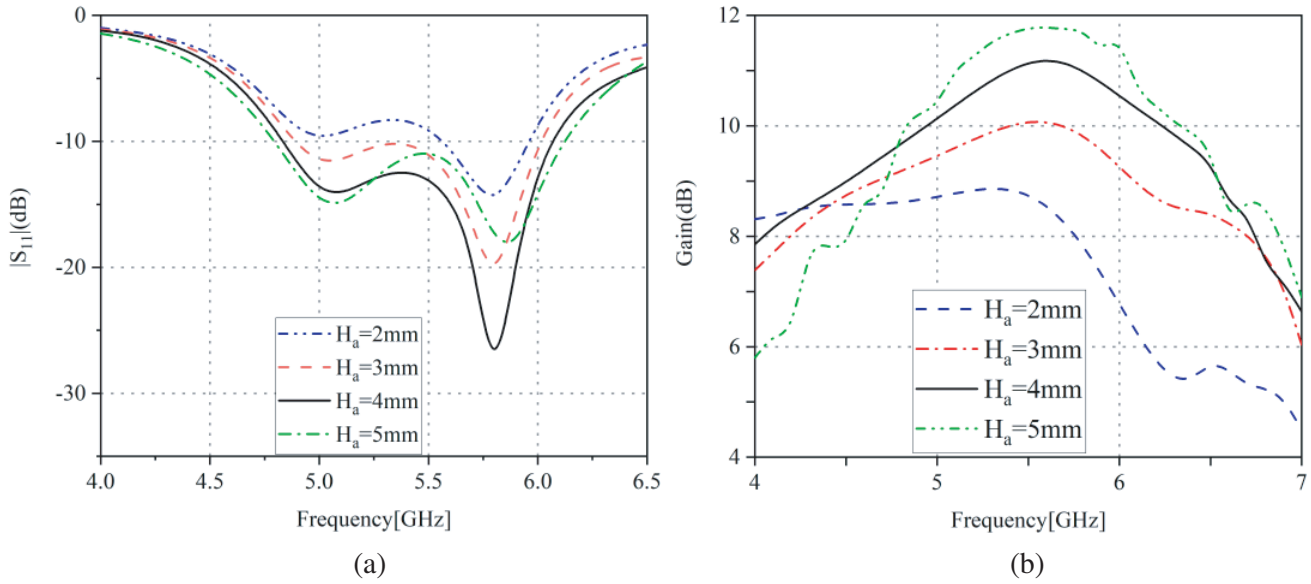

Figure 8. Effect of H_a on the S_{11} and gain performance of the proposed antenna. (a) Impact of H_a on S_{11}. (b) Impact of H_a on Gain.

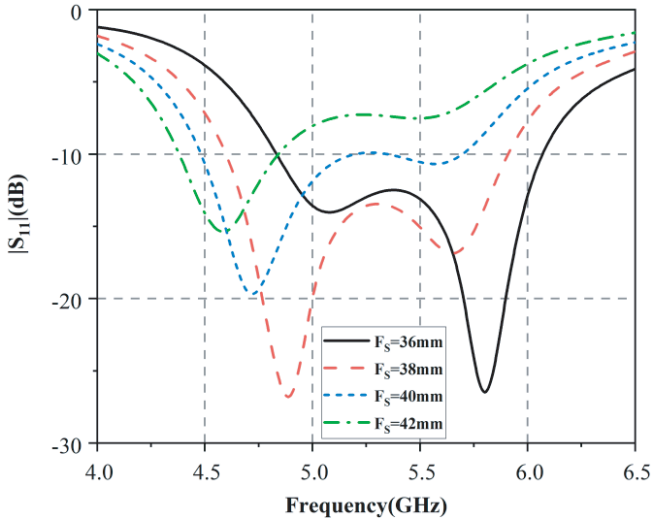

Figure 9. Effect of F_s on the S_{11} performance of the proposed antenna.

When $F_s = 36$ mm, the antenna works at 5.8 GHz; when $F_s = 38$ mm, the antenna works at 4.8 GHz; when $F_s = 40$ mm, the antenna works at 4.6 GHz; when $F_s = 42$ mm, the antenna works at 4.5 GHz. With the increase of the feeder length, the working frequency of the antenna gradually becomes smaller, so changing the feeder length can make the antenna work in different frequency bands. To make the antenna work at WLAN 5.8 GHz, $F_s = 36$ mm is chosen.

2.2.3. Effect of Slot Size

Another major parameter that affects the antenna is slot length S_{L1} and slot width S_{w1}. The effects of different slot lengths on bandwidth performance were studied. Set the value range of S_{L1} to 32–38 mm with a 2 mm interval. The value of S_{W1} ranges from 1 mm to 3 mm with an interval of 1 mm. As shown in Figure 10.

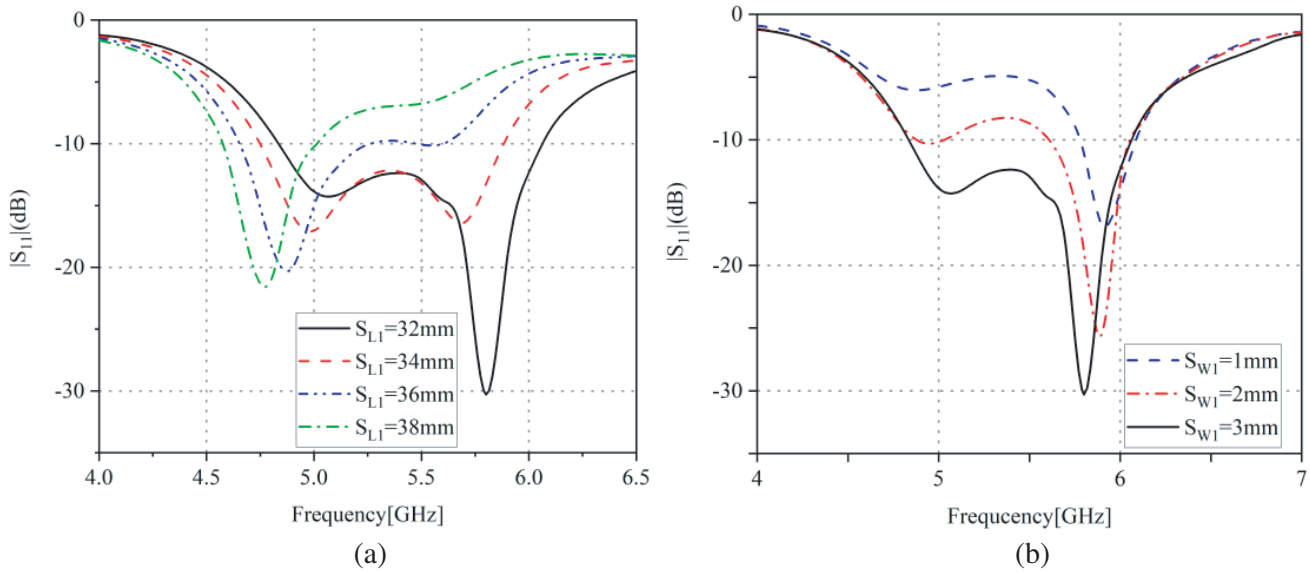

Figure 10. Effect of S_L and S_W on the S_{11} performance of the proposed antenna. (a) Impact of S_{L1} on S_{11}. (b) Impact of S_{w1} on S_{11}.

When $S_{L1} = 32\,\text{mm}$, the antenna works at 5.8 GHz; when $S_L = 34\,\text{mm}$, the antenna works in two frequency bands of 5 GHz and 5.7 GHz; when $S_{L1} = 36\,\text{mm}$, the antenna works at 4.9 GHz; when $S_{L1} = 38\,\text{mm}$, the antenna works at 4.8 GHz. With the increase of the slot length, the working frequency of the antenna gradually becomes smaller, that is, changing the slot length can make the antenna work in different frequency bands. When $S_{L1} = 32\,\text{mm}$, we get the work bandwidth we need. The effects of different slot widths on antenna bandwidth are also studied. When $S_{w1} = 1\,\text{mm}$, the antenna works at 5.9 GHz; when $S_{w1} = 2\,\text{mm}$, the antenna works at 5.9 GHz; when $S_{w1} = 3\,\text{mm}$, the antenna works at

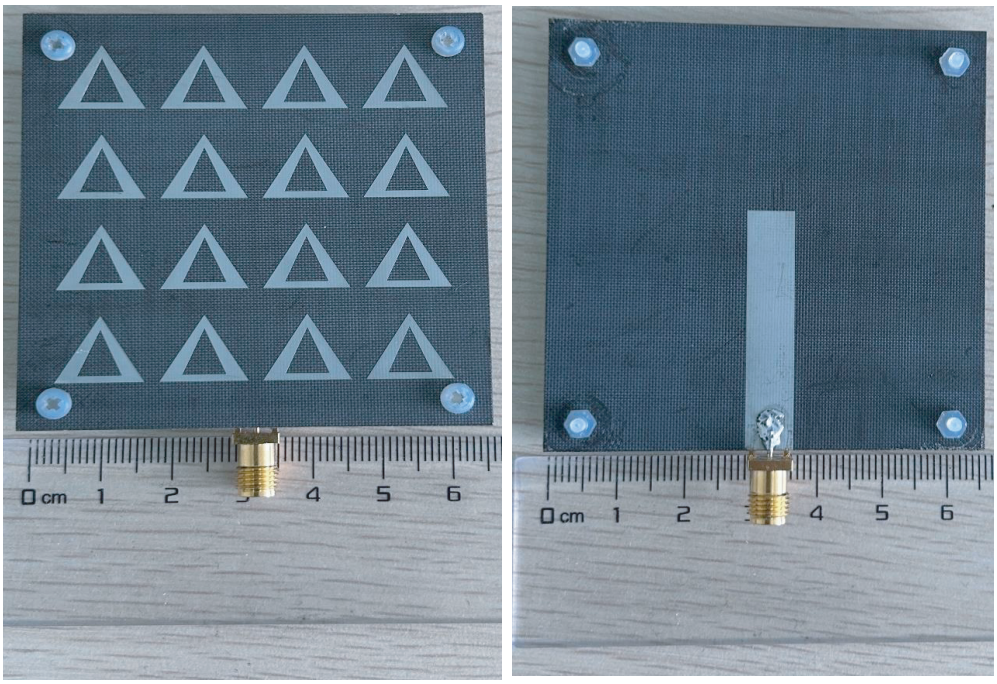

(a) (b)

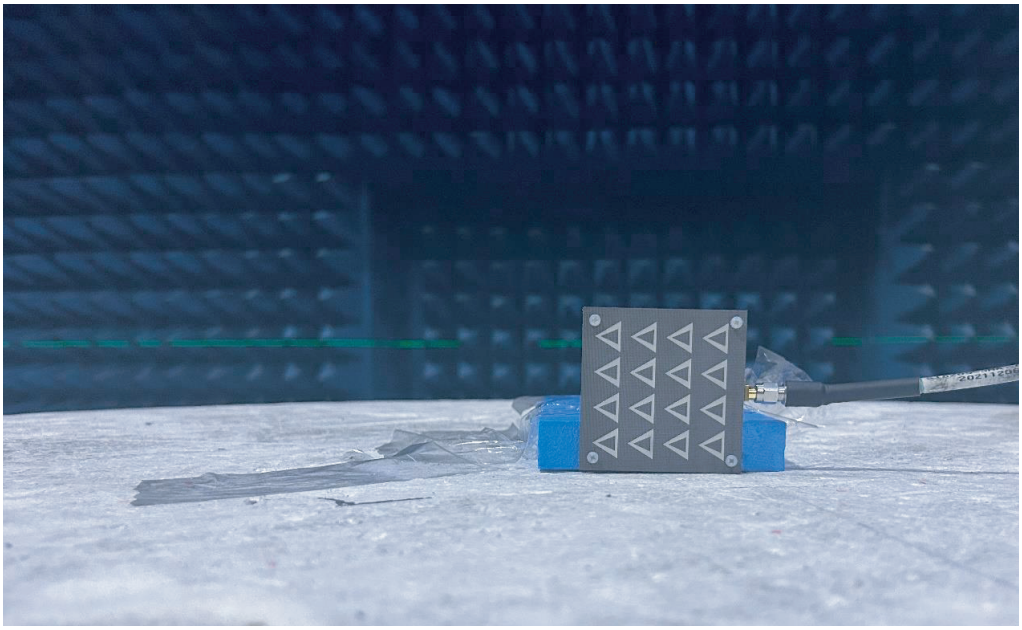

(c)

Figure 11. Antenna model and test environment. (a) Top view. (b) Bottom view. (c) Test environment.

5.8 GHz. With the increase of the slot width, the working frequency of the antenna gradually decreases, and the best matching is obtained when $S_{w1} = 3$ mm. According to the above analysis, it is found that the antenna's working frequency can be changed by adjusting the slot length and slot width. Based on the above analysis, $S_{L1} = 32$ mm and $S_{w1} = 3$ mm are the best parameters to make the antenna work the best.

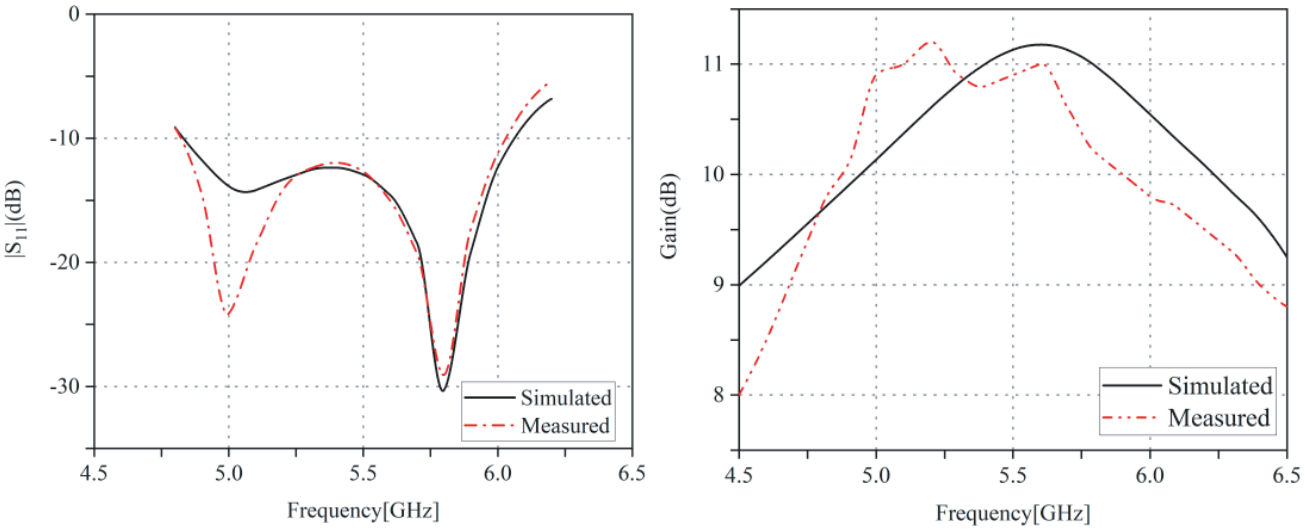

Figure 12. Simulated and measured S_{11} and gain of the modified antenna. (a) S_{11}. (b) Gain.

3. RESULTS AND DISCUSSION

To verify the proposed antenna design, the prototype antenna was processed, measured, and analyzed. The antenna size is the same as proposed above. Figure 11 shows the photos of the antenna prototype and testing environment. The two boards are of the same size, both of which are 64 mm×64 mm×1.5 mm. Figure 12 provides the simulated and measured reflection coefficients and gains of the antenna, respectively.

The simulated −10 dB bandwidth is 4.8–6.1 GHz, with a gain range of 9.6–10.3 dB and a peak gain of 11.2 dB at 5.6 GHz. The measurement range of −10 dB impedance bandwidth is 4.8–6.1 Hz, and there is a good match at 5 GHz. The measurement range of gain is 9.7–9.6 dB, reaching a peak of 11.2 dB at 5.2 GHz. This may be due to the antenna processing accuracy and connector SMA, including possible contact and welding technical problems during welding, and there may be some slight errors between the actual gain and simulation gain, but this error is not significant and belongs to a normal and acceptable range.

In general, the simulated results agree well with the measured ones. The radiation patterns of this antenna at 5.8 GHz in the working band are shown in Figure 13. Desirable radiations are obtained at the frequency point. From Figure 13, good agreements are observed between the measurement and simulation results.

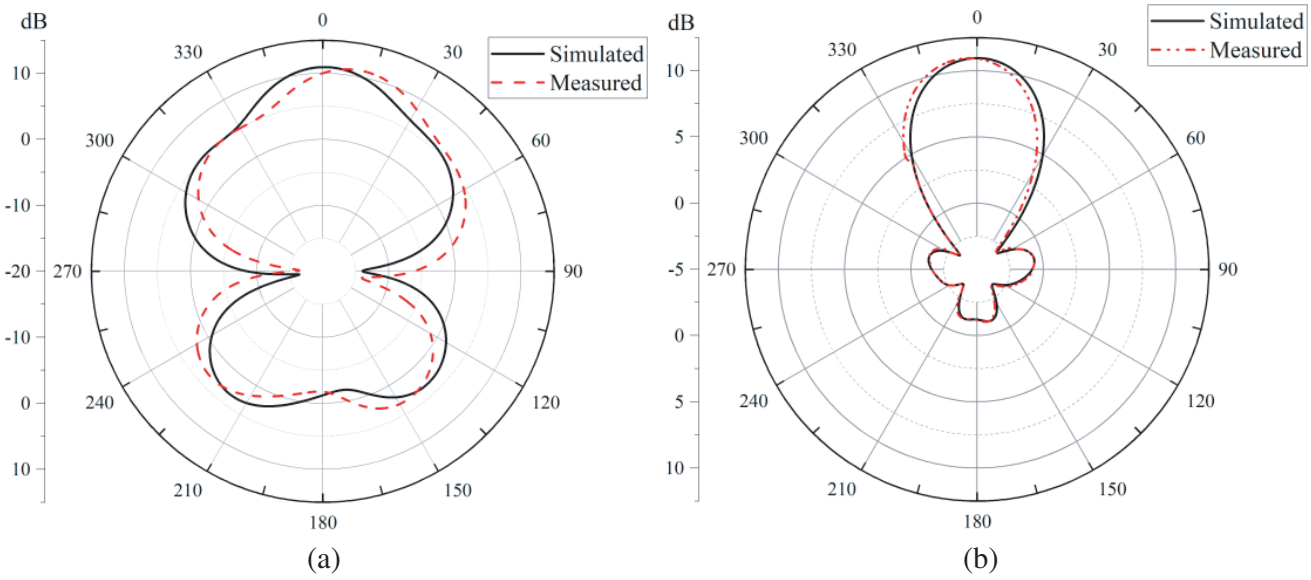

Figure 13. Simulated and measured radiation patterns of (a) *E*-plane at 5.8 GHz, (b) *H*-plane at 5.8 GHz.

4. CONCLUSION

A triangular toroidal metasurface wideband high gain patch antenna is proposed. The performance of without slotting metasurface, traditional rectangular metasurface, non-loaded metasurface, and the metasurface antenna proposed in this paper are compared and analyzed. The changes in various parameters on the antenna performance are also simulated and analyzed. This antenna works at 4.8–6.1 GHz, and its gain can be well maintained at 10 dB, which is relatively stable. Measurement results validate the design, and it can be used in the WLAN band. This antenna has a potential application in the WLAN band where wideband, simple design, and the high-gain planar antenna are required. Through the simulation analysis, it is possible to use other structures to replace the influence of triangular metasurface simulation on antenna performance, which has a good basic impact on the development of metasurface antennas in the future.

ACKNOWLEDGMENT

This work was supported in part by the National Natural Science Foundation of China under Grant 62202372; the Young Talent Fund of the University Association for Science and Technology in Shaanxi, China under Grant 20200111; Key Research and Development Plan of Shaanxi Province (General project) under Grant 2023-YBGY-038; Shaanxi Key Laboratory of Space Extreme Detection Fund under Grant SED20221203; The Program for Talent of Colleges and Universities Service Enterprise of Xi'an under Grant 23GXFW0061.

REFERENCES

1. Chaturvedi, D., A. Kumar, and S. Raghavan, "Wideband HMSIW-based slotted antenna for wireless fidelity application," *IET Microw. Antenna. P.*, Vol. 13, No. 2, 258–262, 2019.
2. Li, Y. J., Z. Y. Lu, and L. S. Yang, "CPW-fed slot antenna for medical wearable applications," *IEEE Access*, Vol. 7, 42107–42112, 2019.
3. Yi, X. and H. Wong, "Wideband substrate integrated waveguide fed open slot antenna array," *IEEE Access*, Vol. 8, 74167–74174, 2020.
4. Ali, A., H. Wang, Y. Yun, J. Lee, and I. Park, "Compact slot antenna integrated with a photovoltaic cell," *J. Electromagn. Eng. Sc.*, Vol. 20, No. 4, 248–253, 2020.
5. Cui, T. J., L. Li, S. Liu, Q. Ma, L. Zhang, X. Wan, W. X. Jiang, and Q. Cheng, "Information metamaterial systems," *Iscience*, Vol. 23, No. 8, 2020.
6. Wan, W., M. Xue, L. Cao, T. Ye, and Q. Wang, "Low-profile broadband patch-driven metasurface antenna," *IEEE Antenn. Wirel. Pr.*, Vol. 19, No. 7, 1251–1255, 2020.
7. Liu, S., D. Yang, Y. Chen, K. Sun, X. Zhang, and Y. Xiang, "Low-profile broadband metasurface antenna under multimode resonance," *IEEE Antenn. Wirel. Pr.*, Vol. 20, No. 9, 1696–1700, 2021.
8. Liu, S., D. Yang, and J. Pan, "A low-profile broadband dual-circularly-polarized metasurface antenna," *IEEE Antenn. Wirel. Pr.*, Vol. 18, No. 7, 1395–1399, 2019.
9. Kedze, K. E., H. Wang, and I. Park, "A metasurface-based wide-bandwidth and high-gain circularly polarized patch antenna," *IEEE T. Antenn. Propag.*, Vol. 70, No. 1, 732–737, 2021.
10. Badawe, M. E., T. S. Almoneef, and O. M. Ramahi, "A true metasurface antenna," *Sci. Rep.-UK*, Vol. 6, No. 1, 19268, 2016.
11. Nie, N. S., X. S. Yang, Z. N. Chen, and B. Z. Wang, "A low-profile wideband hybrid metasurface antenna array for 5G and WiFi systems," *IEEE T. Antenn. Propag.*, Vol. 68, No. 2, 665–671, 2019.
12. Wang, J., H. Wong, Z. Ji, and Y. Wu, "Broadband CPW-fed aperture coupled metasurface antenna," *IEEE Antenn. Wirel. Pr.*, Vol. 18, No. 3, 517–520, 2019.
13. Meriche, M. A., H. Attia, A. Messai, S. S. I. Mitu, and T. A. Denidni, "Directive wideband cavity antenna with single-layer meta-superstrate," *IEEE Antenn. Wirel. Pr.*, Vol. 18, No. 9, 1771–1774, 2019.
14. Olawoye, T. O. and P. Kumar, "A high gain antenna with DGS for sub-6 GHz 5G communications," *Adv. Electromagn.*, Vol. 11, No. 1, 41–50, 2022.
15. Yang, Z. Z., F. Liang, Y. Yi, D. Zhao, and B. Z. Wang, "Metasurface-based wideband, low-profile, and high-gain antenna," *IET Microw. Antenna. P.*, Vol. 13, No. 4, 436–441, 2019.
16. Cao, Y., Y. Cai, W. Cao, B. Xi, Z. Qian, T. Wu, and L. Zhu, "Broadband and high-gain microstrip patch antenna loaded with parasitic mushroom-type structure," *IEEE Antenn. Wirel. Pr.*, Vol. 18, No. 7, 1405–1409, 2019.
17. Liu, S., D. Yang, Y. Chen, K. Sun, X. Zhang, and Y. Xiang, "Low-profile broadband metasurface antenna under multimode resonance," *IEEE Antenn. Wirel. Pr.*, Vol. 20, No. 9, 1696–1700, 2021.
18. Chen, D., Q. Xue, W. Yang, K. S. Chin, H. Jin, and W. Che, "A compact wideband low-profile metasurface antenna loaded with patch-via-wall structure," *IEEE Antenn. Wirel. Pr.*, Vol. 22, No. 1, 179–183, 2022.
19. Kedze, K. E., H. Wang, and I. Park, "A metasurface-based wide-bandwidth and high-gain circularly polarized patch antenna," *IEEE T. Antenn. Propag.*, Vol. 70, No. 1, 732–737, 2021.